Reduced rate of adenosine triphosphate synthesis by *in vivo* ^{31}P nuclear magnetic resonance spectroscopy and downregulation of PGC-1ß in distal skeletal muscle following burn

A. ARIA TZIKA[1,2], DIONYSSIOS MINTZOPOULOS[1,2], KATIE PADFIELD[1], JULIE WILHELMY[3], MICHAEL N. MINDRINOS[3], HONGUE YU[1,2], HAIHUI CAO[1,2], QUNHAO ZHANG[1], LOUKAS G. ASTRAKAS[1,2], JIANGWEN ZHANG[4], YONG-MING YU[1], LAURENCE G. RAHME[1] and RONALD G. TOMPKINS[1]

[1]Department of Surgery, Massachusetts General Hospital and Shriners Burn Institute, Harvard Medical School, Boston, MA 02114; [2]Athinoula A. Martinos Center of Biomedical Imaging, Department of Radiology, Massachusetts General Hospital, Boston, MA 02114; [3]Department of Biochemistry, Stanford University School of Medicine, Stanford, CA 94305; [4]Bauer Center for Genomics Research, Harvard University, Cambridge, MA 02138, USA

Received September 10, 2007; Accepted October 19, 2007

Abstract. Using a mouse model of burn trauma, we tested the hypothesis that severe burn trauma corresponding to 30% of total body surface area (TBSA) causes reduction in adenosine triphosphate (ATP) synthesis in distal skeletal muscle. We employed *in vivo* ^{31}P nuclear magnetic resonance (NMR) in intact mice to assess the rate of ATP synthesis, and characterized the concomitant gene expression patterns in skeletal muscle in burned (30% TBSA) versus control mice. Our NMR results showed a significantly reduced rate of ATP synthesis and were complemented by genomic results showing downregulation of the ATP synthase mitochondrial F_1F_0 complex and PGC-1ß gene expression. Our findings suggest that inflammation and muscle atrophy in burns are due to a reduced ATP synthesis rate that may be regulated upstream by PGC-1ß. These findings implicate mitochondrial dysfunction in distal skeletal muscle following burn injury. That PGC-1ß is a highly inducible factor in most tissues and responds to common calcium and cyclic adenosine monophosphate (cAMP) signaling pathways strongly suggests that it may be possible to develop drugs that can induce PGC-1ß.

Introduction

When burn injury exceeds 30% of the total body surface area (TBSA), local inflammation generalizes into a severe systemic response metabolically characterized as muscle catabolism, leading to muscle wasting or 'cachexia' (1). While early burn wound excision has been shown to favorably influence the metabolic response and reduce catabolism (2), administration of appropriate factors that can change post-burn physiology would also be a powerful tool for ameliorating 'cachexia'. Although the clinical consequences for a patient with an extensive burn injury are grave, the mechanisms underpinning post-burn metabolic alterations and muscle catabolism remain uncertain. *In vivo* nuclear magnetic resonance (NMR) spectroscopy allows measurements of physiological biomarkers in intact systems and has recently shown mitochondrial dysfunction in local burns (3). In addition, the application of microarrays has greatly advanced physiological studies by providing a snapshot of the transcriptome in a specific organ. Combining NMR and microarray data enables functional genomics studies to be performed and validated.

Recent studies have revealed a novel mode of regulation for many complex biological programs, including metabolism by coactivator proteins, best illustrated by the peroxisome proliferator-activated receptor coactivator 1 (PPARγ coactivator-1 or PGC-1) family of coactivators (4,5). The first member of the PGC-1 family was identified from brown adipose tissue as a PPARγ-interacting protein and is now termed PGC-1α (6). PGC-1ß was identified as the closest homolog of PGC-1α; both share extensive sequence identity (7,8). In general, PGC-1 coactivators play a critical role in the maintenance of glucose, lipid, and energy homeostasis and are likely involved in pathogenic conditions such as neurodegeneration, cardiomyopathy, obesity, diabetes (9), and, presumably, burn injury.

PGC-1ß regulates numerous downstream genes: acyl-Coenzyme A dehydrogenase, medium chain (ACADM); fatty acid synthase (FASN), microsomal triglyceride transfer protein (MTTP); 24-dehydrocholesterol reductase (DHCR24); squalene epoxidase (SQLE); lanosterol synthase (LSS); diacylglycerol O-acyltransferase 1 (DGAT1); farnesyl di-

Correspondence to: Dr A. Aria Tzika, NMR Surgical Laboratory, Department of Surgery, Massachusetts General Hospital, Harvard Medical School, 51 Blossom Street, Room 261, Boston, MA 02114, USA
E-mail: atzika@partners.org

Key words: nuclear magnetic resonance, skeletal muscle, burn trauma, adenosine triphosphate, PGC-1ß, mitochondria

phosphate synthetase (FDPS); glucose-6-phosphatase, catalytic (G6PC); stearoyl-Coenzyme A desaturase 1 (SCD); adenosine triphosphate (ATP) synthase, H^+ transporting mitochondrial F1 complex, ß subunit (ATP5B); cytosolic phosphoenolpyruvate carboxykinase 1 (PCK1); mevalonate (diphospho) decarboxylase (MVD); carnitine palmitoyltransferase 1 (Cpt1); and farnesyl diphosphate farnesyl transferase 1 (FDFT1). It is regulated by host cell factor C1 (HCFC1); retinoblastoma 1 (RB1); and ß-estradiol (10-13). Nuclear respiratory factors (NRF-1 and NRF-2) are among the transcription factors that are targets of the PGC-1α and ß coactivators and regulate the expression of certain nuclear-encoded mitochondrial genes (9). The interplay between PGC-1α and forkhead box O (FoxO) family transcription factors has been reported, and the decrease in PGC-1α in muscle atrophy was suggested to enhance a FoxO-dependent loss of muscle mass (14). A possible interplay between PGC-1ß and FoxO has not as yet been suggested.

The first aim of the present study was to evaluate the rate of ATP synthesis in a clinically relevant mouse burn model by employing *in vivo* ^{31}P NMR. Our second aim was to characterize the concomitant gene expression patterns in the skeletal muscle of burned versus intact control mice. We hypothesize that PGC-1ß regulates ATP synthesis and mitochondrial function in burn injury. Because PGC-1ß is a highly inducible factor in most tissues and responds to common calcium and cyclic adenosine monophosphate (cAMP) signaling pathways, it is a promising pharmaceutical target.

Materials and methods

Experimental animals. Male, 6-week-old CD1 mice, weighing ~20-25 g, were purchased from Charles River Laboratory (Boston, MA). The animals were maintained on a regular light-dark cycle (lights on from 8 am to 8 pm) at an ambient temperature of 22±1˚C and had free access to food and water. All animal experiments were approved by the Subcommittee on Research Animal Care of Massachusetts General Hospital, Boston, MA.

TBSA (30%) burn model. Prior to receiving burn injury, mice were anesthetized by intraperitoneal injection of 40 mg/kg pentobarbital sodium and were randomly divided into burn and control groups. The total surface area of each mouse was calculated using Meeh's formula ($A = k \times W^{2/3}$ where A = surface area in cm^2; k = proportionality constant 12.3 and W = weight in g). To standardize the surface area burned, templates were produced for various animal weights. Mice were laid supine in the template so that the skin protruding from the template represented 30% TBSA. The protruding skin was immersed for 8 sec in water at 90˚C. Mice were resuscitated with a 2-ml intraperitoneal injection of 0.9% sterile saline. After injury, animals were given analgesia in the form of buprenorphine 0.05-0.1 mg/kg SQ, as required. This burn model was previously established (15,16) and is considered to be clinically relevant.

^{31}P NMR spectroscopy. Animals were studied with *in vivo* ^{31}P NMR spectroscopy 1, 3, and 7 days after burn trauma. The mice were transiently anesthetized using a nose cone and vaporizer with a halothane/oxygen mixture (5% for induction, 1% for maintenance), and placed in a customized restraining tube. The left hind limb was placed into a solenoid coil (4 turns, length 2 cm, diameter 1 cm) tuned to the ^{31}P frequency (162.1 MHz). The rectal body temperature was maintained at 37±1˚C using heated water blankets. All *in vivo* ^{31}P NMR experiments were performed in a horizontal bore magnet (proton frequency at 400 MHz, 21 cm diameter, Magnex Scientific) using a Bruker Avance console. Field homogeneity was adjusted using the ^{1}H signal of tissue water. A 90˚ pulse was optimized for detection of phosphorus spectra (repetition time 2 sec, 400 averages, 4K data points). Saturation 90˚-selective pulse trains (duration 36.534 msec, bandwidth 75 Hz) followed by crushing gradients were used to saturate the γ-ATP peak. The same saturation pulse train was also applied downfield of the inorganic phosphate (P_i) resonance, symmetrically to the γ-ATP resonance. T1 relaxation times of P_i and phosphocreatine (PCr) were measured using an inversion recovery pulse sequence in the presence of γ-ATP saturation. An adiabatic pulse (400 scans, sweep with 10 KHz, 4K data) was used to invert P_i and PCr, with an inversion time between 152 and 7651 msec. The theoretical basis of saturation transfer experiments and calculations has been described by Forsen and Hoffman (17).

^{31}P NMR spectra were analyzed using the MestRe-C NMR software package (Mestrelab Research, NMR solutions, www.mestrec.com). Free induction decays were zero filled to 8K points and apodized with exponential multiplication (20 Hz) before Fourier transformation. The spectra were then manually phased and corrected for baseline broad features. The Levenberg-Marquardt algorithm was used to least-square-fit a model of mixed Gaussian/Lorentzian functions to the data. Similarly, the T_{1obs} relaxation time for P_i and PCr was calculated by fitting the function $y = A_1(1 - A_2e^{-(t/Tobs)})$ to the inversion recovery data, where y is the z magnetization and t is the inversion time.

Extraction of RNA. Biopsies from the left gastrocnemius muscle (distal to the burn injury) were harvested at 6 h, 12 h, 1 day, 3 days, or 7 days post-burn (n=3 for each time point) to examine changes in whole muscle gene expression. The mice were anesthetized by intraperitoneal injection of 40 mg/kg pentobarbital, and the muscle specimens were excised and immediately immersed in 1 ml Trizol® (Gibco BRL, Invitrogen, Carlsbad, CA) for RNA extraction. All mice were then administered a lethal dose of pentobarbital by intraperitoneal injection (200 mg/kg). Each muscle specimen was homogenized for 60 sec with a Brinkman Polytron 3000 before extraction of total RNA. Chloroform (200 µl) was added to the homogenized muscle and mixed by inverting the tube for 15 sec. After centrifugation at 12,000 g for 15 min, the upper aqueous phase was collected and precipitated by adding 500 µl isopropanol. Further centrifugation at 12,000 g for 10 min separated the RNA pellet, which was then washed with 500 µl of 70% ethanol and centrifuged at 7500 g for 5 min prior to air drying. The pellet was re-suspended in 100 µl DEPC-H_20. An RNeasy Kit (Qiagen, MD, USA) was used to purify the RNA according to the manufacturer's protocol. Purified RNA was quantified by UV absorbance at

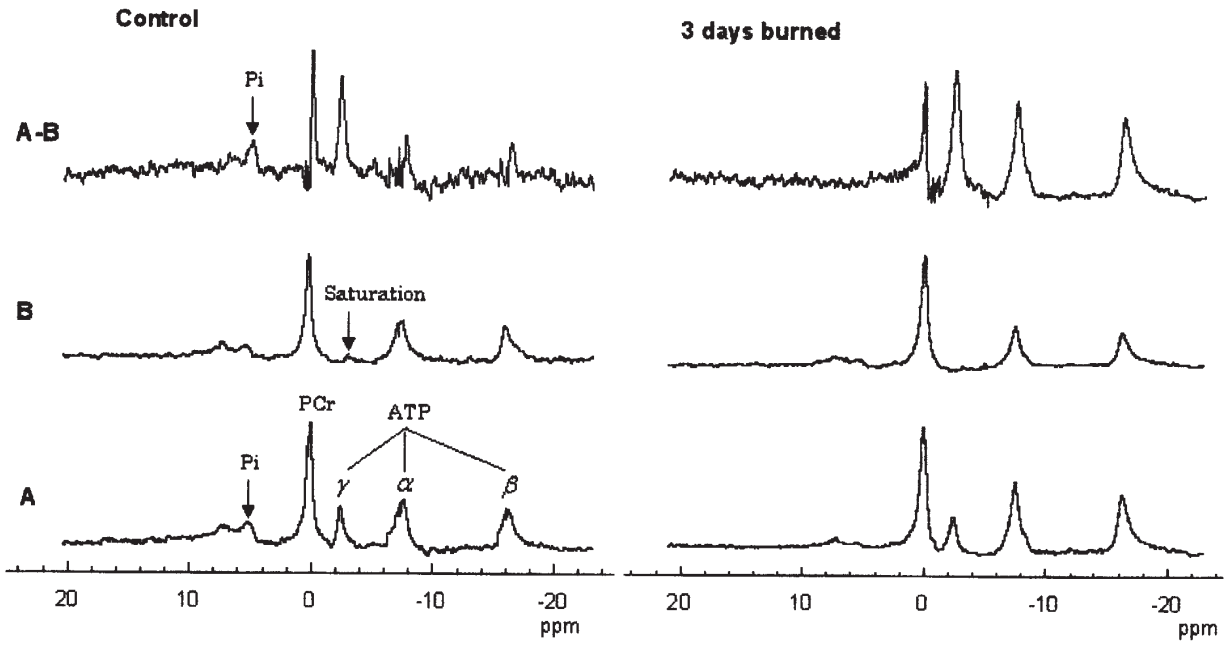

Figure 1. NMR spectra of *in vivo* ^{31}P-NMR saturation-transfer performed on the hind limb skeletal muscle of conscious mice. The spectra were acquired from control and burned mice three days post-burn before (A) and after (B) saturation of the γ-ATP resonance. The difference spectra between the two are also shown (A-B). The arrow indicates the position of the saturation by RF irradiation of the γ-ATP resonance (P_i is an inorganic phosphate).

260 and 280 nm and stored at -70˚C for DNA microarray analysis.

Microarray hybridization. Biotinylated cRNA was generated with 10 μg of total cellular RNA according to the protocol outlined by Affymetrix Inc. (Santa Clara, CA, USA). The cRNA was hybridized onto MOE430A oligonucleotide arrays (Affymetrix), stained, washed, and scanned according to the Affymetrix protocol.

Genomic data analysis. Data files of the scanned image files hybridized with probes from RNA extracted from the gastrocnemius isolated at the specified times from burned or control mice (n=2) were converted to cell intensity files (.CEL files) with the Microarray suite 5.0 (MAS, Affymetrix). The data were scaled to a target intensity of 500, and all possible pairwise array comparisons of the replicates to normal control mice were performed for each time point (i.e., four combinations when two arrays from each time point were compared to the two arrays hybridized to RNA from control mice) using a MAS 5.0 change call algorithm. Probe sets that had a signal value difference >100 and in which one of the two samples being compared was not called 'absent', were scored as differentially modulated when i) the number of change calls in the same direction were at least 3, 4, and 6 when the number of comparisons were 4, 6, and 9, respectively; and ii) the other comparisons were unchanged. Such scoring was used to partially compensate for biological stochasticity and technical variation. Based on the ratios of 100 genes determined to be invariant in most conditions tested (Affymetrix), an additional constraint of a minimum ratio of 1.65 was applied to control the known false positives at 5%.

Results

Burn injury reduces ATP synthesis rate but not ATP levels or PH in distal skeletal muscle. Fig. 1 shows representative ^{31}P NMR spectra acquired from normal and burned mice before and after saturation of the γ-ATP resonance, and their difference spectrum (Fig. 1A and B). The mean results are presented in Table I. Upon irradiation of the γ-ATP resonance, the signal intensities of PCr, P_i, α-ATP, and ß-ATP resonances all decreased, either by magnetization transfer or direct off-resonance saturation. The fractional change $\Delta M/M_0$ decreased by 43.7, 64.2, and 81.8% at 1, 3, and 7 days post-burn, respectively (percent change in $\Delta M/M_0$, Table I). The fractional change $\Delta M/M_0$ and the observed spin lattice relaxation time (T_{1obs}) were used to calculate the rate constant using the equation:

$$\kappa_f = \frac{1}{T_{1obs}} \times \frac{\Delta M_{(P_i)}}{M_{0(P_i)}} \qquad (1)$$

which, when multiplied by the P_i concentration, gives ATP synthesis flux. The unidirectional flux of the reaction $P_i \rightarrow$γ-ATP was significantly reduced by 78.3, 90.7, and 98.1% at 1, 3, and 7 days post-burn, respectively. Although burn also was seen to reduce the flux of the reaction PCr→γ-ATP by 42.3%, this reduction was statistically insignificant. Fig. 2 is a graphic representation of the *in vivo* ^{31}P-NMR saturation transfer experiments and shows that the ATP synthesis rate exponentially decayed post-burn.

Burn injury downregulates the expression of oxidative phosphorylation-related genes in skeletal muscle. In our

Table I. Results of *in vivo* ^{31}P-NMR saturation transfer experiments performed on the hind limb skeletal muscle of conscious mice.

	Baseline	1 day post-burn	3 days post-burn	7 days post-burn
$\Delta M/M_0$	0.318±0.025	0.179±0.052[a] (-43.7%)	0.114±0.030[a] (-64.2%)	0.058±0.004[a] (-81.8%)
$T1_{obs}$ (sec)	1.13±0.24	2.42±0.64	3.22±0.50	3.9
K (sec^{-1})	0.281±0.022	0.074±0.022[a]	0.035±0.009[a]	0.015±0.001[a]
P_i (μmol/g)	0.574±0.250	0.443±0.191[b]	0.425±0.202[b]	0.193±0.014[c]
Flux (μmol/g/sec)	0.161±0.069	0.035±0.026[c] (-78.3%)	0.015±0.010[a] (-90.7%)	0.003±0.0004[a] (-98.1%)

ATP synthesis flux (reaction $P_i \rightarrow \gamma$-ATP); $\Delta M/M_0$, the fractional change in P_i magnetization as a result of saturation transfer; T_{1obs}, observed spin lattice relaxation time of P_i during γ-ATP saturation in sec; K, rate constant. ATP synthesis is calculated as $[P_i] \times K$. A bioluminescence assay kit was used to assess ATP concentration. [a]P<0.001 versus control values; [b]P<0.05 versus control values; [c]P<0.05 versus control values (Student's t-test).

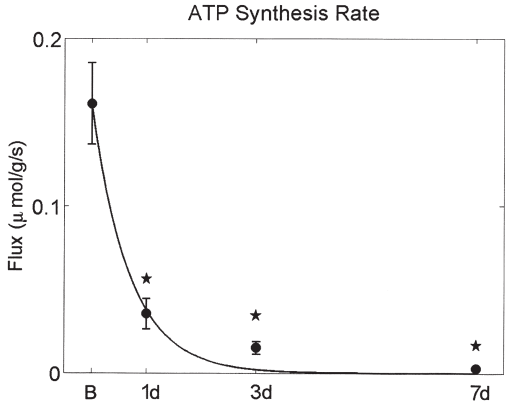

Figure 2. ATP synthesis flux (μmol/g/sec) after 30% TBSA burn. Data are from *in vivo* ^{31}P-NMR saturation transfer experiments performed on the hind limb skeletal muscle of conscious mice after 30% TBSA burn. Mean values are shown in black squares; error bars correspond to standard errors. Data were fitted with an exponential decay (solid line) using standard nonlinear fitting procedures in Matlab (MathWorks, Inc., Natick, MA). The characteristic rate of the exponential decay equals 1.4531 [(μmol/g/sec)/d]. The χ^2 of the fit equals 1.8614×10^{-4} (a perfect errorless fit is χ^2=0). *P<0.001 for B compared to 1 day; P<0.001 for B compared to 3 days; and P<0.001 for B compared to 7 days (Student's t-test); B, baseline.

transcriptome studies, we compared the expression of all genes that might lead to metabolic dysfunction in skeletal muscle after a burn. Fig. 3 shows the profiles of differentially expressed genes involved in oxidative metabolism at 5 time points following 30% TBSA burn. Burn trauma upregulated the gene for pyruvate dehydrogenase kinase 4 from 6 h to 1 day post-injury. The downstream TCA cycle genes, including pyruvate dehydrogenase (lipoamide) ß, succinate dehydrogenase subunits, and citrate synthase were not differentially expressed in the 30% TBSA burn condition. However, malate dehydrogenase, the final enzyme of the TCA cycle, was upregulated at all time points (Fig. 3). Also, several components of the mitochondrial respiratory chain were downregulated in the 30% TBSA burn condition, including subunits of NADH dehydrogenases and ATP synthase (F_1F_0 ATPase or complex V).

Burn injury downregulates the expression of the PGC-1ß gene and affects the expression of other key regulatory genes in skeletal muscle. Figs. 4 and 5 show that the expression of the PGC-1ß and Irs1 (insulin substrate) genes was significantly reduced after 30% TBSA burn. The differential expression of

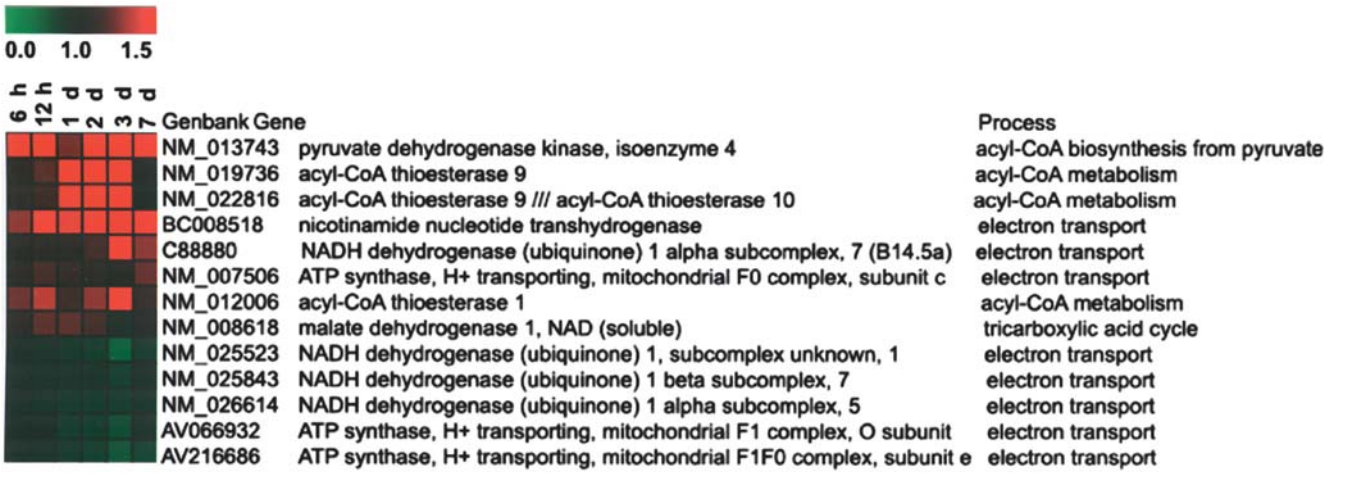

Figure 3. Differentially expressed genes involved in oxidative metabolism at five time points following 30% TBSA burn. Red boxes represent upregulation of the gene and green boxes represent downregulation of the gene compared with normal muscle. The expression of certain key genes such as ATP synthase is downregulated, consistent with the *in vivo* ^{31}P NMR data (Figs. 1 and 2).

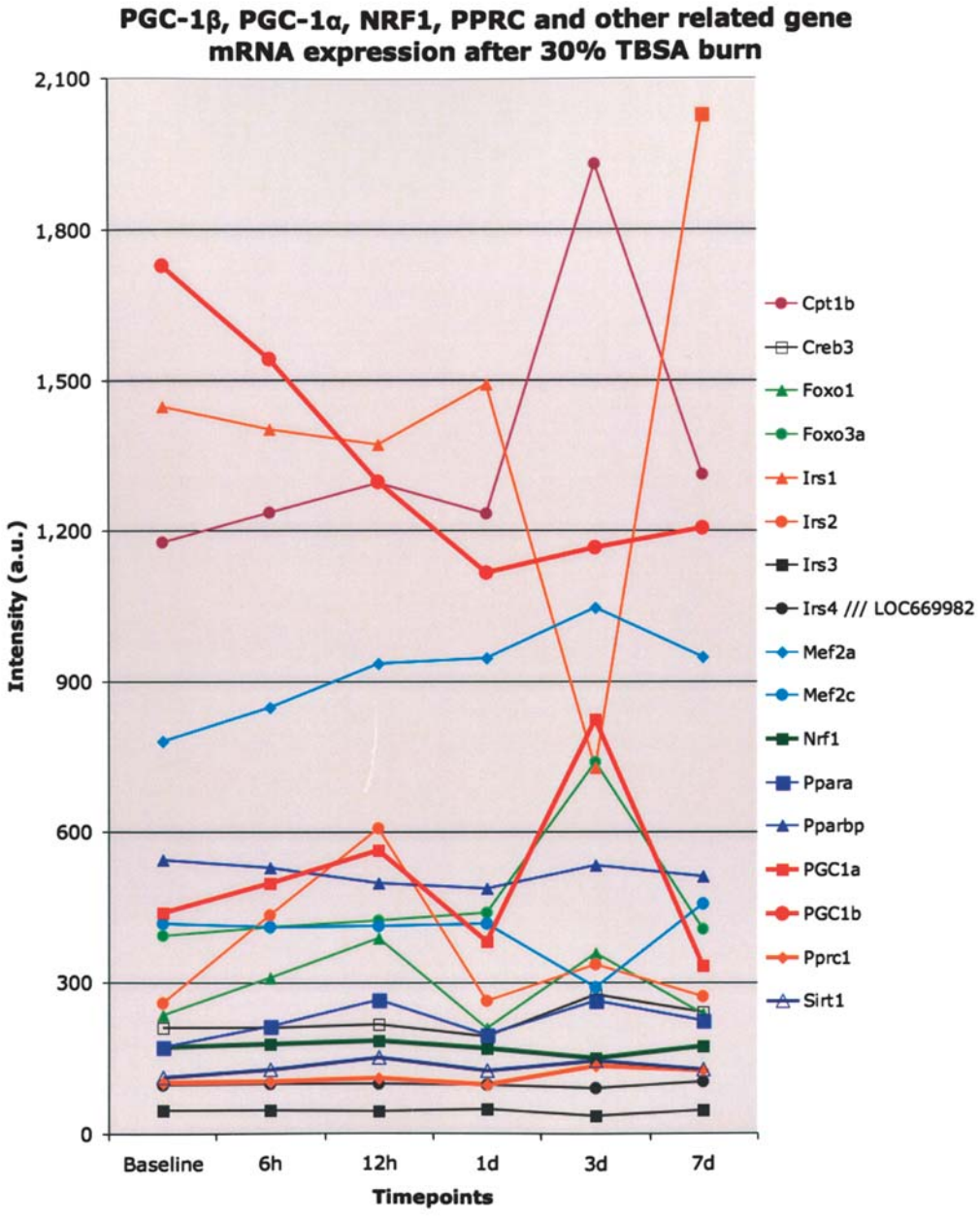

Figure 4. PGC-1ß, PGC-1α, NRF1, PPRC and other related gene mRNA expression after 30% TBSA burn. The expression of PGC-1ß was significantly downregulated starting at 6 h and sustained for at least 7 days post-burn. Downregulation of PGC-1ß gene expression paralleled reduction in the ATP synthesis rate according to NMR (Figs. 1 and 2). In addition, the expression of Irs1 (insulin substrate) was significantly reduced by 3 days post-burn and increased thereafter. The expression of PGC-1α, Pcpt1ß, and FoxO3α exhibited non-significant compensatory increases at 3 days post-burn. The expression of other related genes did not change.

other relevant genes such as PGC-1α and NRF was not significantly altered. PGC-1α only exhibited a compensatory increase at 3 days. Notably, the expression of FoxO3α peaked at 3 days post-burn. Fig. 5 shows that, of the genes that PGC-1ß regulates, only the expression of Fdft1 and Dgat1 was significantly altered at 3 days. The expression of Rb1, which regulates PGC-1ß was significantly increased at 3 days.

Discussion

The present study demonstrated that burn trauma reduces the ATP synthesis rate in distal skeletal muscle while triggering a downregulation of ATP synthase and other oxidative phosphorylation genes as well as PGC-1ß mRNA. The downregulation in PGC-1ß expression in skeletal muscle following local burn, which parallels the ATP synthesis rate reduction, may be an upstream regulatory mechanism involving mitochondrial uncoupling and leading to apoptosis as observed in burned skeletal muscle (18,19). Such a process may occur in response to increased levels of cytokines [e.g., TNFα in systemic burn (20) causes downregulation of PGC-1 as observed in liver cells (21)]. Our findings suggest a more general role for PGC-1ß in skeletal muscle metabolism, implicating it in inflammation, diabetes, and obesity.

Our *in vivo* ^{31}P-NMR saturation-transfer spectra data showed that burn trauma reduces ATP synthesis in a manner that is consistent with a reduction in the rate of mitochondrial phosphorylation, as *in vivo* ^{31}P-NMR saturation-transfer can

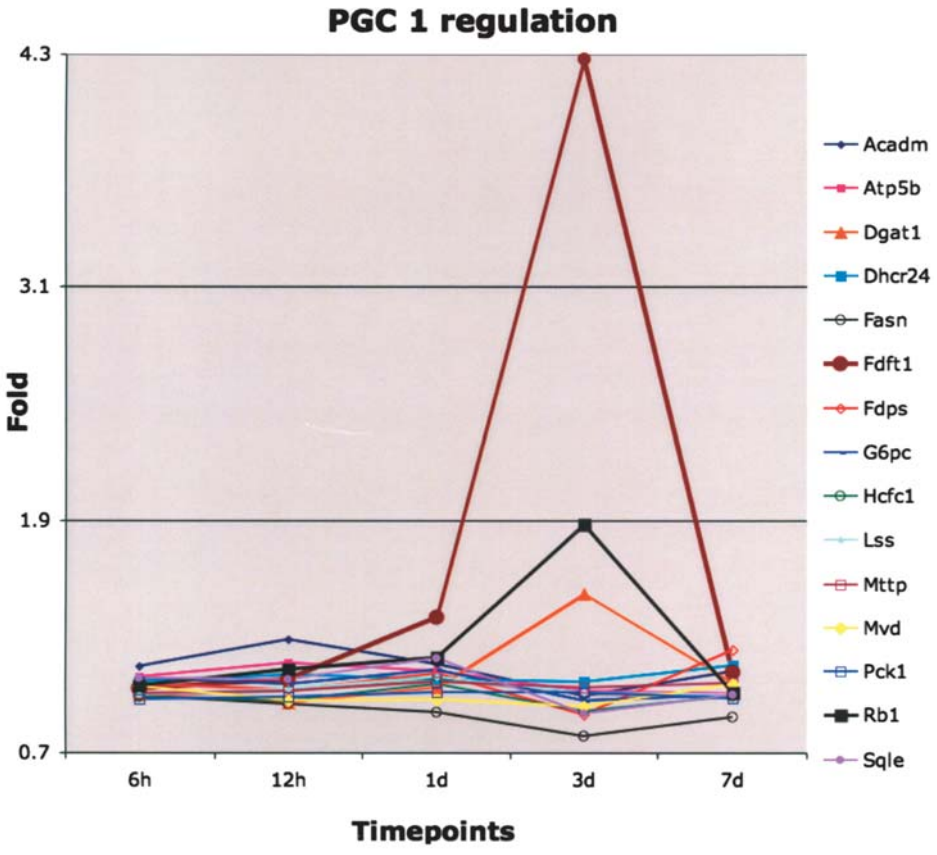

Figure 5. PGC-1ß regulation. PGC-1ß regulates ACADM, FASN, MTTP, DHCR24, SQLE, LSS, DGAT1, FDPS, G6PC, SCD, ATP5B, PCK1, MVD, Cpt1, and FDFT1 genes and is regulated by HCFC1, RB1, and ß-estradiol. However, only the expression of Fdft1, Dgat1, and Rb1, was significantly altered at 3 days post-burn.

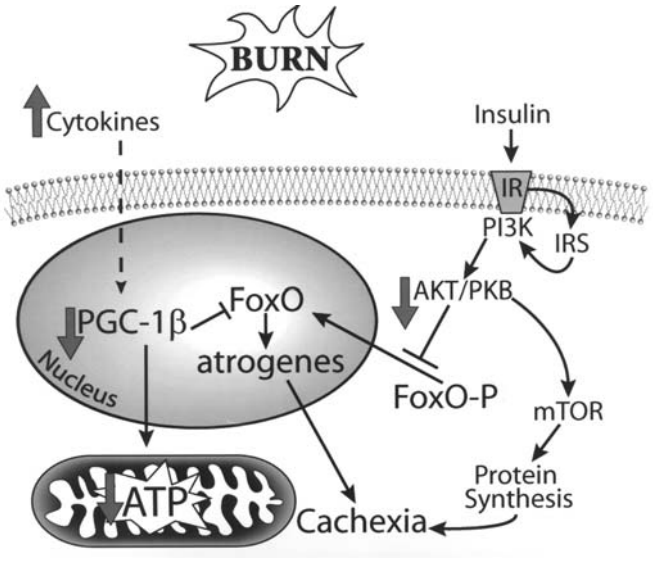

Figure 6. Mechanism for muscle atrophy induced by burn and the role of PGC-1ß. Following burn, significant downregulation of PGC-1ß expression causes dysregulation of mitochondria, resulting in reduced ATP synthesis. Also, it does not inhibit translational activity of FoxO3, which normally suppresses atrogen expression and proteolysis, leading to muscle atrophy or 'cachexia'. In addition, the insulin-stimulated phosphorylation of AKT/PKB is significantly attenuated (28). Thus, AKT does not phosphorylate FoxO and, via mTOR, does not contribute to protein synthesis, which also results in 'cachexia'. PGC-1ß probably affects IRS expression (not indicated here) and thus insulin resistance in skeletal muscle. IR, insulin receptor; IRS, insulin receptor substrate; PI3K, phosphatidylinositol 3-kinase; FoxO3, forkhead box O3.

non-invasively measure fast enzyme reaction exchange rates (22). Furthermore, under appropriate conditions, this technique (23,24) can measure the net rate of oxidative ATP synthesis catalyzed by mitochondrial ATPase in skeletal muscle, which is proportional to the oxygen consumption rate by the P:O ratio (the ratio of the net rate of ATP synthesis by oxidative phosphorylation to the rate of oxygen consumption) (25,26). Other investigators have proposed that the NMR-measured unidirectional ATP synthesis flux primarily reflects flux through F_1F_0-ATP synthase, with negligible influence of the coupled glyceraldehyde-3-phosphate dehydrogenase and phosphoglycerate kinase reactions (24). Although the net glycolytic contribution of glyceraldehyde-3-phosphate dehydrogenase and phosphoglycerate kinase to ATP production is small compared with that of oxidative phosphorylation, these enzymes occur at near equilibrium, and thus the unidirectional production of ATP can be high. Since burn injury down-regulates glycolytic enzyme gene expression, we assume that the contribution of glycolytic reactions to the unidirectional ATP synthesis flux is negligible.

Another novel finding of our experiments consistent with the observed ATP production is that burn trauma down-regulates the expression of PGC-1ß in the first 6 h post-burn, and that the downregulation is sustained for at least 7 days post-burn (Fig. 4). It has been reported that the activity of ATP-consuming reactions was increased in cells expressing PGC-1ß (27). The expression profile of Irs1, which was significantly reduced by 3 days and increased thereafter, may

suggest that PGC-1ß affects Irs1 expression and thus insulin resistance in skeletal muscle. If this is the case, then PGC-1ß could contribute to the insulin resistance caused by burn. A different pathway through attenuation of Akt has been also proposed (28). In burn, the phosphorylation of Akt is inhibited and thus Akt does not phosphorylate FoxO1, 3, and 4, which would normally suppress atrogen expression and proteolysis. In addition, Akt would normally contribute to protein synthesis via mTOR, but attenuation of Akt leads to inhibition of protein synthesis and cachexia (29). These findings, together with recent published reports (14,28,30), suggest that these two mechanisms, which may involve an increase in FoxO3 expression, may account for muscle wasting and cachexia observed in burned patients (Fig. 6). Thus in this study, a similar interplay reported between PGC-1α and FoxO family transcription factors (14) is suggested between PGC-1ß and FoxO.

Our transcriptome findings suggest that burn trauma results in reduced ATP synthesis by muscle mitochondria, which is validated by our *in vivo* NMR spectroscopy results. Further, downregulation of PGC-1ß gene expression may lead to the mitochondrial dysfunction that underlies skeletal muscle wasting and general cachexia in burn pathophysiology (31). It has been shown that PGC-1ß like PGC-1α increases mitochondrial biogenesis and respiration when expressed in muscle cells, implicating the importance of this gene in mitochondrial metabolism (27). In addition, it has recently been recognized as an activator of uncoupling proteins (UCPs) (9,27,32). Whether PGC-1ß has a role in mitochondrial uncoupling in burn trauma needs to be investigated using *in vivo* assessment by NMR, which is superior to electric potential measurements across the inner mitochondrial membrane (33). Nevertheless, the expression of UCPs may be stimulated by PGC-1s, and UCPs seem to greatly reduce reactive oxygen species (ROS) production by the mitochondria (9). Thus, we propose that downregulation of PGC-1ß observed in this study leaves the muscle unprotected against the harmful oxidative damage of ROS, which is probably exacerbated by burn.

The upregulation of Fdft1 and Dgat1 by 3 days post-burn may be a consequence of PGC-1ß downregulation in burn trauma since these two genes are regulated upstream by PGC-1ß. This means that the cholesterol and/or lipid biosynthetic processes and acyltransferase activity at the endoplasmic reticulum, controlled by Fdft1 and Dgat1 respectively, are upregulated in this setting. Although the significance of these findings is not yet clear, we suggest that lipids and proteins may be used as alternative sources to glucose in 30% TBSA burn trauma. Also, that Rb1 is increased 3 days post-burn is consistent with the down-regulation of PGC-1ß at this time point. Since Rb1 negatively affects PGC-1ß gene expression (13), the increased expression of Rb1 at 3 days post-burn may contribute to the sustained downregulation of PGC-1ß. Thus, for the first time, we propose a role for Rb1 in mitochondrial dysfunction following burn besides its role in striated muscle cell differentiation, transcription, and negative regulation of cell proliferation.

Finally, not only is burn trauma in our mouse model comparable to common burn injuries in humans, but our findings may be clinically relevant inasmuch as the activity of PGC-1ß may be induced. Indeed, recent clinical studies indicated that PGC-1α agonists can alleviate post-burn insulin resistance (34,35) and prevent burn-induced damage in remote organs (36). That PGC-1ß is a highly inducible factor in most tissues and responds to common pathways of calcium and cAMP signaling strongly suggests that it may be possible to find drugs that induce PGC-1ß. Furthermore, these findings open a door to a better understanding of the physiological and pathological processes attendant to systemic burn trauma and suggest that further experiments exploring the role of PGC-1ß in a variety of inflammatory situations in which PGC-1ß agonists may have protective effects should be pursued.

Acknowledgements

This work was supported in part by a Shriner's Hospital for Children research grant (no. 8893) to A. Aria Tzika, a National Institute Institutes of Health (NIH) Center Grant (no. P50GM021700) to Ronald G. Tompkins and by a NIH Center Grant to the Stanford Genome Technology Center. Qunhao Zhang was a Shriners Research Fellow. We also thank Dr Zenab Amin and Dr Ann Power Smith of Write Science Right for their editorial assistance.

References

1. Sheridan RL and Tompkins RG: What's new in burns and metabolism. J Am Coll Surg 198: 243-263, 2004.
2. Barret JP and Herndon DN: Modulation of inflammatory and catabolic responses in severely burned children by early burn wound excision in the first 24 hours. Arch Surg 138: 127-132, 2003.
3. Padfield KE, Astrakas LG, Zhang Q, *et al*: Burn injury causes mitochondrial dysfunction in skeletal muscle. Proc Natl Acad Sci USA 102: 5368-5373, 2005.
4. Spiegelman BM and Heinrich R: Biological control through regulated transcriptional coactivators. Cell 119: 157-167, 2004.
5. Handschin C and Spiegelman BM: Peroxisome proliferator-activated receptor gamma coactivator 1 coactivators, energy homeostasis, and metabolism. Endocr Rev 27: 728-735, 2006.
6. Puigserver P, Wu Z, Park CW, Graves R, Wright M and Spiegelman BM: A cold-inducible coactivator of nuclear receptors linked to adaptive thermogenesis. Cell 92: 829-839, 1998.
7. Kressler D, Schreiber SN, Knutti D and Kralli A: The PGC-1-related protein PERC is a selective coactivator of estrogen receptor alpha. J Biol Chem 277: 13918-13925, 2002.
8. Lin J, Puigserver P, Donovan J, Tarr P and Spiegelman BM: Peroxisome proliferator-activated receptor gamma coactivator 1beta (PGC-1beta), a novel PGC-1-related transcription coactivator associated with host cell factor. J Biol Chem 277: 1645-1648, 2002.
9. Lin J, Handschin C and Spiegelman BM: Metabolic control through the PGC-1 family of transcription coactivators. Cell Metab 1: 361-370, 2005.
10. Kamei Y, Ohizumi H, Fujitani Y, *et al*: PPARgamma coactivator 1beta/ERR ligand 1 is an ERR protein ligand, whose expression induces a high-energy expenditure and antagonizes obesity. Proc Natl Acad Sci USA 100: 12378-12383, 2003.
11. Lin J, Tarr PT, Yang R, *et al*: PGC-1beta in the regulation of hepatic glucose and energy metabolism. J Biol Chem 278: 30843-30848, 2003.
12. Lin J, Yang R, Tarr PT, *et al*: Hyperlipidemic effects of dietary saturated fats mediated through PGC-1beta coactivation of SREBP. Cell 120: 261-273, 2005.
13. Hansen JB, Jorgensen C, Petersen RK, *et al*: Retinoblastoma protein functions as a molecular switch determining white versus brown adipocyte differentiation. Proc Natl Acad Sci USA 101: 4112-4117, 2004.

14. Sandri M, Lin J, Handschin C, *et al*: PGC-1alpha protects skeletal muscle from atrophy by suppressing FoxO3 action and atrophy-specific gene transcription. Proc Natl Acad Sci USA 103: 16260-16265, 2006.
15. Schildt B and Nilsson A: Standardized burns in mice. Eur Surg Res 2: 23-33, 1970.
16. Walker HL and Mason AD Jr: A standard animal burn. J Trauma 8: 1049-1051, 1968.
17. Forsen S and Hoffman R: Study of moderately rapid chemical exchange reactions by means of nuclear magnetic double resonance. J Chem Phys 39: 2892, 1963.
18. Yasuhara S, Perez ME, Kanakubo E, *et al*: Skeletal muscle apoptosis after burns is associated with activation of proapoptotic signals. Am J Physiol Endocrinol Metab 279: E1114-E1121, 2000.
19. Astrakas LG, Goljer I, Yasuhara S, *et al*: Proton NMR spectroscopy shows lipids accumulate in skeletal muscle in response to burn trauma-induced apoptosis. FASEB J 19: 1431-1440, 2005.
20. Maass DL, Hybki DP, White J and Horton JW: The time course of cardiac NF-kappaB activation and TNF-alpha secretion by cardiac myocytes after burn injury: contribution to burn-related cardiac contractile dysfunction. Shock 17: 293-299, 2002.
21. Kim MS, Sweeney TR, Shigenaga JK, *et al*: Tumor necrosis factor and interleukin 1 decrease RXRalpha, PPARalpha, PPARgamma, LXRalpha, and the coactivators SRC-1, PGC-1alpha, and PGC-1beta in liver cells. Metabolism 56: 267-279, 2007.
22. Alger JR and Shulman RG: NMR studies of enzymatic rates *in vitro* and *in vivo* by magnetization transfer. Q Rev Biophys 17: 83-124, 1984.
23. Brindle KM, Blackledge MJ, Challiss RA and Radda GK: 31P NMR magnetization-transfer measurements of ATP turnover during steady-state isometric muscle contraction in the rat hind limb *in vivo*. Biochemistry 28: 4887-4893, 1989.
24. Jucker BM, Dufour S, Ren J, *et al*: Assessment of mitochondrial energy coupling *in vivo* by 13C/31P NMR. Proc Natl Acad Sci USA 97: 6880-6884, 2000.
25. Sako EY, Kingsley-Hickman PB, From AH, Foker JE and Ugurbil K: ATP synthesis kinetics and mitochondrial function in the postischemic myocardium as studied by 31P NMR. J Biol Chem 263: 10600-10607, 1988.
26. Kingsley-Hickman PB, Sako EY, Ugurbil K, From AH and Foker JE: 31P NMR measurement of mitochondrial uncoupling in isolated rat hearts. J Biol Chem 265: 1545-1550, 1990.
27. St-Pierre J, Lin J, Krauss S, *et al*: Bioenergetic analysis of peroxisome proliferator-activated receptor gamma coactivators 1alpha and 1beta (PGC-1alpha and PGC-1beta) in muscle cells. J Biol Chem 278: 26597-26603, 2003.
28. Sugita H, Kaneki M, Sugita M, Yasukawa T, Yasuhara S and Martyn JA: Burn injury impairs insulin-stimulated Akt/PKB activation in skeletal muscle. Am J Physiol Endocrinol Metab 288: E585-E591, 2005.
29. Wullschleger S, Loewith R and Hall MN: TOR signaling in growth and metabolism. Cell 124: 471-484, 2006.
30. Zhang Q, Carter EA, Ma BY, White M, Fischman AJ and Tompkins RG: Molecular mechanism(s) of burn-induced insulin resistance in murine skeletal muscle: role of IRS phosphorylation. Life Sci 77: 3068-3077, 2005.
31. Yu YM, Tompkins RG, Ryan CM and Young VR: The metabolic basis of the increase in energy expenditure in severely burned patients. JPEN J Parenter Enteral Nutr 23: 160-168, 1999.
32. Puigserver P, Rhee J, Lin J, *et al*: Cytokine stimulation of energy expenditure through p38 MAP kinase activation of PPARgamma coactivator-1. Mol Cell 8: 971-982, 2001.
33. Cline GW, Vidal-Puig AJ, Dufour S, Cadman KS, Lowell BB and Shulman GI: *In vivo* effects of uncoupling protein-3 gene disruption on mitochondrial energy metabolism. J Biol Chem 276: 20240-20244, 2001.
34. Cree MG, Zwetsloot JJ, Herndon DN, *et al*: Insulin sensitivity and mitochondrial function are improved in children with burn injury during a randomized controlled trial of fenofibrate. Ann Surg 245: 214-221, 2007.
35. Cree MG, Newcomer BR, Herndon DN, *et al*: PPAR-alpha agonism improves whole body and muscle mitochondrial fat oxidation, but does not alter intracellular fat concentrations in burn trauma children in a randomized controlled trial. Nutr Metab 4: 9, 2007.
36. Sener G, Sehirli AO, Gedik N and Dulger GA: Rosiglitazone, a PPAR-gamma ligand, protects against burn-induced oxidative injury of remote organs. Burns 33: 587-593, 2007.